Five Generations of Nitroxyl-Functionalized Dendrimers

A. W. Bosman, R. A. J. Janssen,* and E. W. Meijer

The Laboratory of Organic Chemistry, Eindhoven University of Technology, P.O. Box 513, 5600 MB Eindhoven, The Netherlands

Received February 10, 1997; Revised Manuscript Received April 9, 1997[⊗]

ABSTRACT: The preparation and electron paramagnetic resonance (EPR) spectroscopy of a series of fully functionalized poly(propylene imine) dendrimers (DAB-*dendr*-$(NH_2)_n$; n = 2, 4, 8, 16, 32, 64) with 3-carboxy-2,2,5,5-tetramethyl-1-pyrrolidinyloxy radical end groups is described. The pendant nitroxyl end groups exhibit a strong exchange interaction. As a consequence, the EPR spectrum directly reveals the number of end groups from the splitting between the hyperfine transitions for the lower generations. For the higher generations an increasingly exchanged−narrowed EPR spectrum is observed. The temperature and solvent dependency of the exchange interaction is used to assess the dynamic behavior of the dendritic branches. FT-IR spectroscopy shows that a hydrogen-bonded network between the amide functionalities is present, consistent with the observed solvent effect on the EPR spectra.

I. Introduction

Combination of the globular structure of dendrimers with functional properties is one of the focal points of current research in dendritic molecules.[1] This interest is motivated by the recognition that the controlled branching of dendritic structures may provide a three-dimensional architecture that allows functional groups to be incorporated in a geometrically well-defined fashion. The low polydispersity and nanoscopic dimensions of well-defined functionalized dendrimers may give rise to new properties in, for example, molecular recognition, catalysis, or molecule-based electronics and optics. Functional properties can be introduced at (i) the core of the dendrimer,[2−5] (ii) as an intrinsic element of the dendritic branches,[6,7] (iii) as pendant groups at the dendrimer surface, or (iv) as noncovalently bound encapsulated guests.[8]

An increasing number of dendrimers are being functionalized with stable organic radicals or redox active groups, aiming at molecules or materials with a wide variety of functional properties. Living radical polymerization of vinyl monomers has been performed with different generations of poly(benzyl ether) dendrons attached to a stable nitroxyl radical core.[9] High-spin molecules formed from organic radicals incorporated into a π-conjugated hyperbranched topology have been studied in relation to future organic magnetic materials.[10−12] In these molecules, dendritic branching is used to ensure a more robust intramolecular spin alignment than can be obtained in linear or branched structures. The electrical conductivity of poly(amido amine) dendrimers with naphthalene diimide anion radical end groups, forming π-dimers or π-stacks, has been reported.[13] Redox active end groups such as tetrathiafulvenyl and ferrocenyl have been attached at the periphery of dendrimers as pendant groups. In these cases, multielectron oxidation to the corresponding cations could be accomplished, but no evidence was obtained for a significant interaction between the end groups.[14−16]

The interaction between pendant functional groups at the exterior of the dendritic surface and their dynamic behavior is of fundamental importance for understanding the properties of dendrimers. In analogy to their linear macromolecular counterparts, the dynamic behavior of pendant end groups and their mutual interactions can be probed using electron paramagnetic resonance (EPR) spectroscopy when the functional groups are stable radicals.[17] Here we describe a first example of five generations of dendrimers with stable radical end groups. A series of poly(propylene imine) dendrimers (DAB-*dendr*-$(NH_2)_n$; n = 2, 4, 8, 16, 32, 64) functionalized with 3-carboxy-2,2,5,5-tetramethyl-1-pyrrolidinyloxy (3-carboxy-PROXYL) radicals (Scheme 1, for n = 2 and 16) has been prepared and studied in detail using EPR spectroscopy.[18] The individual nitroxyl radicals at the exterior of the DAB-*dendr*-(NH-3-CO-PROXYL)$_n$ dendrimers are found to exhibit a strong exchange interaction, which depends on temperature and solvent and reflects the dynamic behavior of dendritic branches.

II. Synthesis

The preparation of different generations of poly(propylene imine) dendrimers has been described elsewhere.[19] For end group functionalization 3-carboxy-2,2,5,5-tetramethyl-1-pyrrolidinyloxy was first activated with *N*-hydroxysuccinimide in 1,2-dimethoxyethane in the presence of 1,3-dicyclohexylcarbodiimide. The DAB-*dendr*-$(NH_2)_n$ dendrimers were subsequently functionalized by reaction with this activated ester (**1**) in dichloromethane (Scheme 1, for n = 2 and 16).[8] The resulting DAB-*dendr*-(NH-3-CO-PROXYL)$_n$ dendrimers, with molecular weights up to 19 kg/mol for the fifth generation, were extensively purified from monoradical impurities using combinations of extraction, column chromatography, and dialysis, depending on the dendrimer generation. The absence of starting material was checked using FT-IR, by monitoring the absence of the C═O stretch vibration of free 3-carboxy-PROXYL (1750 cm^{-1}) and its *N*-hydroxysuccinimide ester (1745 cm^{-1}) and checking for the presence of the amide C═O vibration (1660 cm^{-1}). Simulation of the experimental EPR spectra (*vide infra*) demonstrated that after purification less than 3% monoradical was present for the n = 32 generation of DAB-*dendr*-(NH-3-CO-PROXYL)$_n$ and less than 1% for all other generations. The identity of the DAB-*dendr*-(NH-3-CO-PROXYL)$_n$ dendrimers (n = 2, 4, 8, and 16) was confirmed using matrix-assisted laser desorption and ionization − time of flight (MALDI-TOF) mass spectrometry (Table 1) employing a dithranol (1,8,9-anthracenetriol) matrix. In each case a small deviation between measured and calculated mass (m/z) values has been observed. This mass (m/z) difference

[⊗] Abstract published in *Advance ACS Abstracts,* May 15, 1997.

S0024-9297(97)00185-X CCC: $14.00

Scheme 1

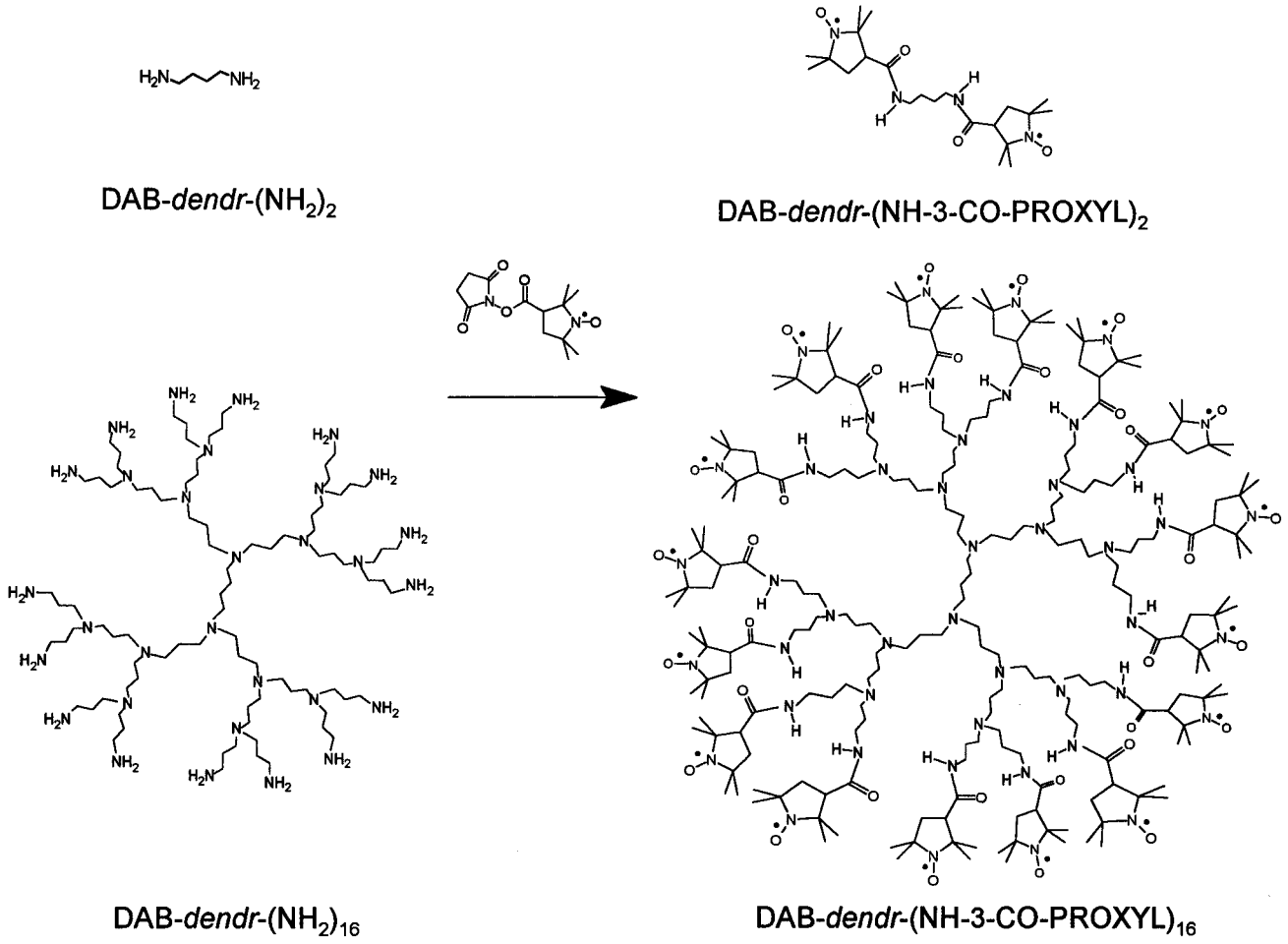

is explained by the partial conversion of the nitroxyl groups to hydroxylamines during sample preparation or ionization. Taking into account that the ionization mechanism, which is protonation in all cases, increases the molecular weight by one mass unit, the number of attached hydrogens is always less than the number of nitroxyl groups. In addition to mass peaks that are due to fragmentation, the MALDI-TOF mass spectra of the nitroxyl-functionalized dendrimers with $n = 8$ and $n = 16$ show peaks at mass (m/z) values due to dendrimers with 7 and 15 nitroxyl groups, respectively, that possibly result from incomplete product formation during the synthesis.

III. EPR and FT-IR Spectroscopy

The EPR spectra of the DAB-*dendr*-(NH-3-CO-PROXYL)$_n$ (n = 2, 4, 8, 16, 32, 64) dendrimers recorded in oxygen-free *N*,*N*-dimethylacetamide at 298 and 378 K are shown in Figure 1. The EPR spectrum of these polyradicals in a nonviscous solvent can be described with a three-term Hamiltonian

$$\hat{\mathbf{H}} = g\mu_B B_0 \sum_{i=1}^{n} \hat{\mathbf{S}}_z^{(i)} + a_N \sum_{i=1}^{n} \hat{\mathbf{I}}_z^{(i)} \cdot \hat{\mathbf{S}}_z^{(i)} - \sum_{i>j=1}^{n} 2J^{(ij)} \hat{\mathbf{S}}^{(i)} \cdot \hat{\mathbf{S}}^{(j)} \tag{1}$$

describing the electron Zeeman interactions, hyperfine coupling a_N, and the exchange interaction J such that when J is negative, the diamagnetic state is the lowest. An important aspect of these polyradicals in solution is the fact that the exchange integrals $J^{(ij)}$ are not constant but a function of the conformation. Therefore the spectrum depends on the temperature, viscosity, and nature of the solvent. Before discussing the spectra of the higher generations, it is instructive to look in some detail at the spectral properties for the biradical (n = 2).

The EPR spectra of nitroxyl biradicals and the influence of the exchange interaction on these spectra have been described in detail theoretically.[20−23] Using the Hamiltonian (eq 1) and the usual singlet $|S\rangle$ and triplet states $|T_+\rangle$, $|T_0\rangle$, $|T_-\rangle$, the four energy levels for a symmetric nitroxyl biradical ($n = 2$) in any nuclear spin state $|m_1 m_2\rangle$ are described by

$$|1\rangle = |T_+\rangle \qquad E_1 = g\mu_B B_0 - {}^1/_2 J + {}^1/_2 a_N (m_1 + m_2) \tag{2}$$

$$|2\rangle = \cos\theta |T_0\rangle + \sin\theta |S\rangle \qquad E_2 = -{}^1/_2 J + {}^1/_2 a_N (m_1 - m_2) \tan\theta$$

$$|3\rangle = -\sin\theta |T_0\rangle + \cos\theta |S\rangle \qquad E_3 = -{}^3/_2 J - {}^1/_2 a_N (m_1 - m_2) \tan\theta$$

$$|4\rangle = |T_-\rangle \qquad E_4 = -g\mu_B B_0 - {}^1/_2 J + {}^1/_2 a_N (m_1 + m_2)$$

Where θ is given by:

$$\tan 2\theta = -a_N (m_1 + m_2)/2J \tag{3}$$

The energies of the transitions and their intensities, obtained by calculating the matrix elements of the $[{}^1/_2(\hat{\mathbf{S}}^+ + \hat{\mathbf{S}}^+)]^2$ operator, are listed in Table 2. From the

Table 1. MALDI-TOF Mass Spectrometry of DAB-*dendr*-(NH-3-CO-PROXYL)$_n$

n	molecular formula	average mass [g/mol] calculated	average mass [g/mol] measured	deviation measured−calculated (g/mol)
2	$C_{22}H_{40}N_4O_4$	424.6	427.2	2.6
4	$C_{52}H_{96}N_{10}O_8$	989.4	992.3	2.9
8	$C_{112}H_{208}N_{22}O_{16}$	2119.0	2123.9	4.9
16	$C_{232}H_{432}N_{46}O_{32}$	4378.3	4386.9	8.6

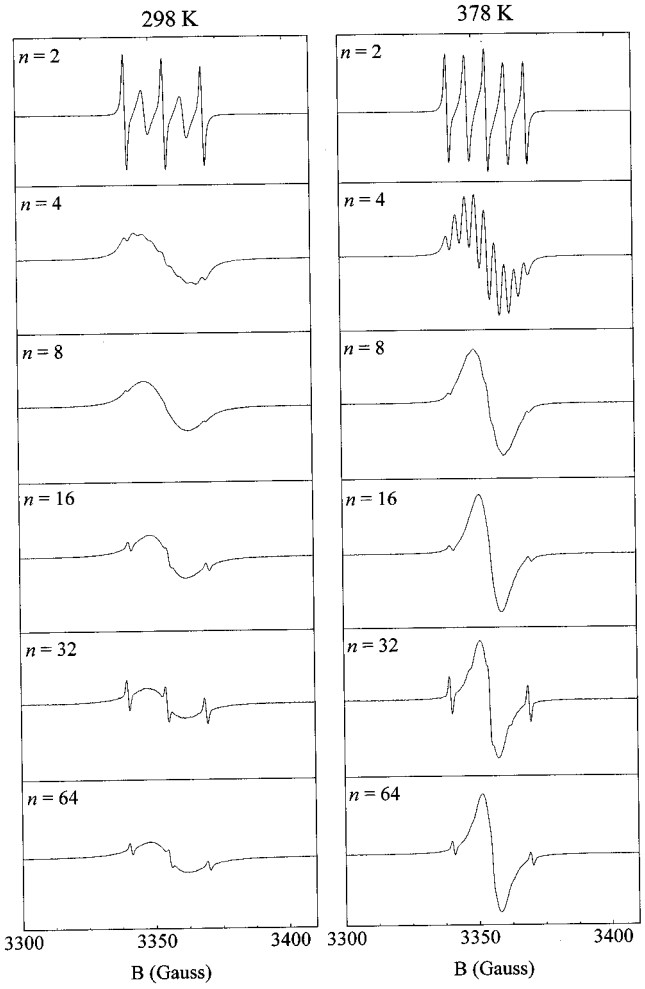

Figure 1. EPR spectra of DAB-*dendr*-(NH-3-CO-PROXYL)$_n$ for n = 2, 4, 8, 16, 32, and 64 in *N*,*N*-dimethylacetamide recorded at 298 and 378 K.

transition energies and their intensities it can be seen that for $|J| \ll |a_N|$ the spectrum of the biradical is similar to that of two independent monoradicals exhibiting three lines separated by a_N with relative intensities 1:1:1. The other possibility, $|J| \gg |a_N|$, gives rise to a five-line hyperfine pattern with a separation of $^1/_2a_N$ and relative intensities of 1:2:3:2:1. These five lines are conveniently labeled with the sum of m_i and m_j (given by $M_I = 2, 1, 0, -1, -2$). At intermediate values, where $|J| \approx |a_N|$, the spectra are more complex.

The experimental EPR spectrum of the DAB-*dendr*-(NH-3-CO-PROXYL)$_2$ biradical recorded at 298 K (Figure 1) exhibits five lines, indicating that $|J| \gg |a_N|$. The widths of the five hyperfine lines clearly alternate. The alternating line width at 298 K and the changes in the spectrum when warming to 378 K result from the modulation of the exchange interaction J, caused by conformational changes of the chain linking the two nitroxyl radicals. The alternating line width and the changes in the spectrum with temperature can be

Table 2. Transitions and Intensities for a Nitroxyl Biradical

transition	energy[a]	intensity[a]
$\|1\rangle \leftrightarrow \|2\rangle$	$g\mu_B B_0 + {}^1/_2a_N(m_1 + m_2) - {}^1/_2a_N(m_1 - m_2)\tan\theta$	$^1/_2\cos^2\theta$
$\|1\rangle \leftrightarrow \|3\rangle$	$g\mu_B B_0 - 2J + {}^1/_2a_N(m_1 + m_2) + {}^1/_2a_N(m_1 - m_2)\tan\theta$	$^1/_2\sin^2\theta$
$\|2\rangle \leftrightarrow \|4\rangle$	$g\mu_B B_0 + {}^1/_2a_N(m_1 + m_2) + {}^1/_2a_N(m_1 - m_2)\tan\theta$	$^1/_2\cos^2\theta$
$\|3\rangle \leftrightarrow \|4\rangle$	$g\mu_B B_0 + 2J + {}^1/_2a_N(m_1 + m_2) - {}^1/_2a_N(m_1 - m_2)\tan\theta$	$^1/_2\sin^2\theta$

[a] θ is defined in eq 3.

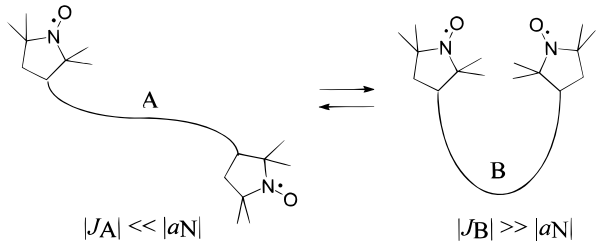

Figure 2. Schematic representation of the nitroxyl biradical DAB-*dendr*-(NH-3-CO-PROXYL)$_2$ with two conformations A and B having different exchange interactions J.

rationalized (albeit in a somewhat naive model) by assuming the presence of at least two classes of conformers, designated schematically with A and B (Figure 2), characterized by strongly different exchange interactions. In an extended structure like A, the exchange integral J is small compared to the ^{14}N hyperfine coupling ($|J_A| \ll |a_N|$), whereas in a conformation with two proximate nitroxyl radicals, such as B, a strong exchange interaction is present ($|J_B| \gg |a_N|$). In solution, both classes of conformers will exist and the actual EPR spectrum depends on the values of J_A and J_B and the rate of interconversion between A and B, expressed by the lifetimes τ_A and τ_B.[20−22] When the exchange interaction is rapidly modulated, the broadening of the line widths due to modulation of J in time is given by[20]

$$T_2^{-1} = \frac{a_N^2 j(2\bar{J})}{16\bar{J}^2}[m_1 - m_2]^2 \qquad (4)$$

where $j(2\bar{J})$ is the spectral density and $\bar{J} = (\tau_A J_A + \tau_B J_B)/(\tau_A + \tau_B)$. This expression shows that of the total of nine nuclear spin functions in a nitroxyl biradical, the three lines corresponding to $m_1 = m_2$ (i.e. $M_I = \pm 2, 0$) are not affected by the modulation of J. In contrast, the widths of the six remaining transitions, for which $m_1 \neq m_2$, are increased. The spectrum exhibits two broader lines for $M_I = \pm 1$ together with a central $M_I = 0$ line (overlapping the sharp central transition) which is broadened by an additional factor of 4. The spectra of DAB-*dendr*-(NH-3-CO-PROXYL)$_2$ clearly correspond to this situation as is demonstrated by simulation of the spectra at 298 and 378 K, using this model with a_N= 14.58 G (Figure 3). Because the line widths of the $M_I = \pm 1$ transitions decrease with increasing temperature, it can be concluded that the modulation of the exchange interaction is fast. If the spectrum at 298 K would correspond to a situation of slow modulation of exchange interaction, the spectrum would be a superposition of the spectra of the individual conformations A and B, and hence an increase in temperature would affect the line widths much less. Moreover, the ratio of the doubly integrated intensities in the experimental spectra is very close to 1:2:3:2:1, confirming our conclusion of fast modulation of exchange interaction.

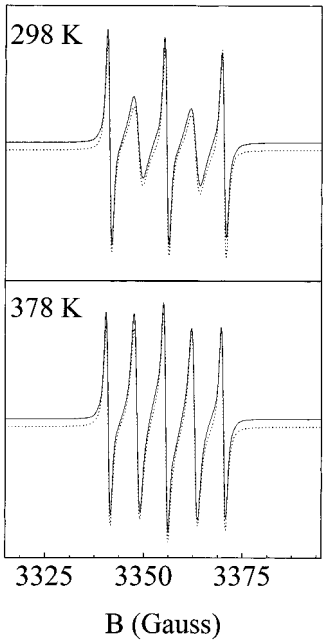

Figure 3. Experimental (solid line) and simulated (dotted line, offset for clarity) EPR spectra of DAB-*dendr*-(NH-3-CO-PROXYL)$_2$.

The spectra of the higher generations and their temperature dependence (Figure 1) show a similar behavior as compared to the biradical. Apart from the polyradical signals, a characteristic nitroxyl 1:1:1 triplet signal of variable intensity is present in each of the spectra. This is attributed to a residual amount of monoradical impurity. Spectral simulation as well as double integration reveals that the amount of nitroxyl monoradicals is less than 3% for $n = 32$ and less than 1% for all other generations. In each case the broadening which is present at room temperature decreases considerably when the temperature is increased to 378 K. For $n = 4$ the spectrum recorded at 378 K clearly shows the expected nine lines separated by $a_N/4$. For $n = 8$ it is possible to discern a number of shoulders, separated by $a_N/8$. For $n = 16$, 32, and 64 the spectral resolution does not allow the observation of the ever-decreasing spacing between the various hyperfine transitions, and the number of nitroxyl radicals can no longer be determined directly from the spectrum. The continuously decreasing peak-to-peak line width (ΔB_{pp}) observed for $n = 16$, 32, and 64, is consistent with the increasing number of nitroxyl end groups. The EPR spectra of these higher generations agree very well with spectral simulations for n nuclei with $I = 1$ ($n = 16$, 32, and 64) having a hyperfine coupling of a_N/n and an EPR line width that is identical to that of the monoradical measured under similar conditions.

The EPR spectra of the DAB-*dendr*-(NH-3-CO-PROXYL)$_n$ dendrimers also depend on the nature of the solvent, as shown in Figure 4 for $n = 4$ and 64. In general, the line widths are smaller in polar solvents such as methanol ($\epsilon = 33.6$) and acetonitrile ($\epsilon = 37.5$) than in more apolar solvents such as toluene ($\epsilon = 2.4$) and dichloromethane ($\epsilon = 9.1$). The fact that the spectrum in *N,N*-dimethylacetamide is broader than expected from its high dielectric constant ($\epsilon = 37.8$) is rationalized by the significantly higher viscosity of this solvent at room temperature ($\eta = 2.14$ mPa·s) as compared to the other solvents ($\eta = 0.3-0.6$ mPa·s). Clearly, the higher viscosity will slow down intramolecular motion and hence the modulation of the

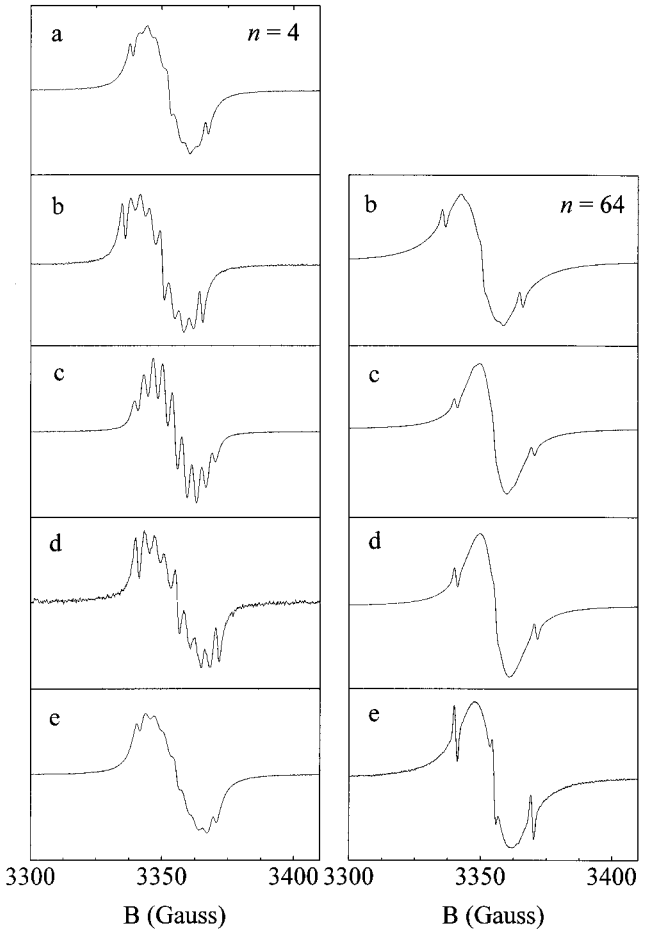

Figure 4. EPR spectra of DAB-*dendr*-(NH-3-CO-PROXYL)$_n$ for $n = 4$ and 64, recorded at room temperature in (a) toluene, (b) dichloromethane, (c) acetonitrile, (d) methanol, and (e) *N,N*-dimethylacetamide. No EPR spectrum for $n = 64$ in toluene could be recorded because of poor solubility.

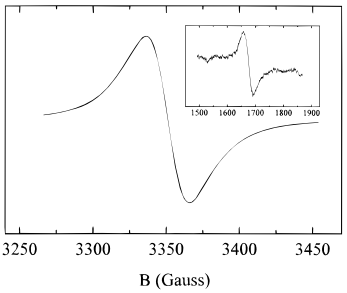

Figure 5. EPR spectrum of DAB-*dendr*-(NH-3-CO-PROXYL)$_{64}$ in dichloromethane, recorded at 120 K. Inset shows the $|\Delta m_s| = 2$ transition at half-field.

exchange interaction. In all solvents investigated, the EPR spectra exhibit a smaller line width at higher temperatures, similar to the behavior shown in Figure 1.

At lower temperatures, the spectra of all dendritic polyradicals continue to broaden. The resulting spectrum for $n = 64$ in dichloromethane at 120 K is shown in Figure 5 as an example and consists of a single and essentially isotropic line with a width of $\Delta B_{pp} = 21$ G. Under these conditions a $|\Delta m_s| = 2$ transition at half-field is observed for each generation, which gives direct evidence of the presence of a high-spin state, exhibiting a zero-field splitting (D). No $|\Delta m_s| = 3$ or other lower-field transitions could be observed. Their absence is in accordance with the fact that the intensity of the $|\Delta m_s| = 1$, 2, and 3 transitions are expected in the ratio 1:(D/

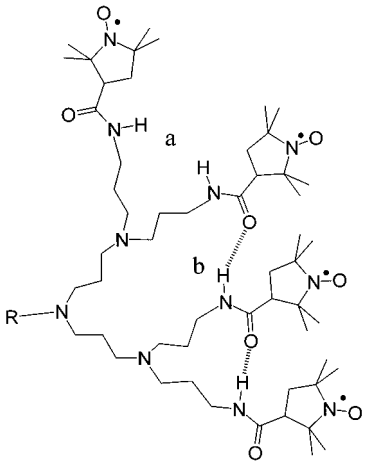

Figure 6. Schematic view of the hydrogen-bonded network in functionalized poly(propylenimine) dendrimers with (a) free NH protons and (b) internal hydrogen (NH···O) bonds.

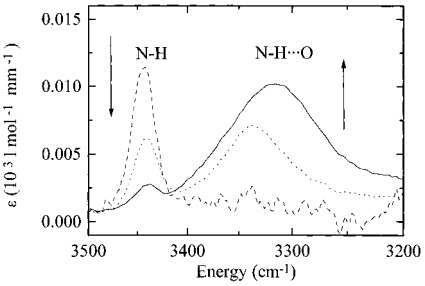

Figure 7. N−H stretch FT-IR spectra of $CH_3CH_2CH_2NH$-3-CO-PROXYL (**2**) (dashed line), DAB-*dendr*-(NH-3-CO-PROXYL)$_4$ (dotted line), and DAB-*dendr*-(NH-3-CO-PROXYL)$_{64}$ (solid line) in CH_2Cl_2 at 298 K, normalized to the number of end groups.

$B_0)^2$:$(D/B_0)^4$.[24] Therefore the $|\Delta m_s| \geq 3$ transitions will go undetected, except when D is large.

The increased flexibility of the dendritic polyradicals in more polar solvents suggests that electric−dipole interactions play a role in the dynamic conformational changes. This observation is consistent with the presence of an intramolecular hydrogen-bonded network for poly(propylene imine) dendrimers where functional end groups are attached via an amide bond (Figure 6). The presence of internal hydrogen bonding has previously been suggested based on various experimental data for higher generations of *N*-(*tert*-butoxycarbonyl)-L-phenylalanine dendrimers, viz. an increase of the spin−lattice relaxation time T_1,[8] the evolution of the NH proton chemical shift,[25] and the vanishing optical activity.[26] The presence of intramolecular hydrogen bonds can also be inferred from FT-IR spectroscopy. The FT-IR spectra of the N−H-stretch region for 0.5−1.5 mM samples of DAB-*dendr*-(NH-3-CO-PROXYL)$_n$ in dichloromethane have been recorded and are shown in Figure 7 for n = 4 and 64 together with the spectrum for the CH_3CH_2-CH_2NH-3-CO-PROXYL monoradical (**2**). The dendrimers give rise to two bands; a narrow band at 3440 cm^{-1} arises from free N-H, and a broad band at 3300−3350 cm^{-1} is due to N-H hydrogen bonded to an amide carbonyl.[27] The FT-IR spectrum of the $CH_3CH_2CH_2NH$-3-CO-PROXYL monoradical (**2**) shows a single N−H stretch at 3440 cm^{-1}, indicating that at the concentrations employed no intermolecular hydrogen bonding occurs. For higher dendrimer generations the band at 3300−3350 cm^{-1}, assigned to intramolecular hydrogen-bonded N−H, increases with respect to the band at 3440 cm^{-1} from non-hydrogen-bonded N−H. For the highest generation, the maximum of the band shifts to lower wavenumbers. These results indicate the progressive formation of an intramolecular hydrogen-bonded network at the periphery of the dendrimers for higher generations, formed by organization of the amide functionalities.

IV. Conclusion

The first five generations of poly(propylene imine) dendrimers have been functionalized with pendant nitroxyl radicals. The nitroxyl radicals at the periphery of the dendrimers exhibit a strong exchange interaction resulting in thermally populated high-spin states. For the lower generations (n = 2, 4, and to some extent 8), the number of transitions in the EPR spectrum and their spacing can be directly related to the number of end groups, confirming the proposed structures. For the higher generations, such an analysis is hampered by the decreasing value of the splitting (a_N/n) and the increasing number of lines ($2n$ +1). In these cases, however, the EPR spectrum gives direct spectral evidence for interaction between the end groups from the progressive exchange narrowing. This result is in contrast with previous studies on dendrimers with paramagnetic end groups in which no interaction[14−16] or formation of a diamagnetic state was observed.[13]

An interesting aspect of the exchange interaction is the fact that it is modulated by the dynamic behavior of the dendritic branches, since they probe conformations with strongly different values of J in time. Since this modulation of the exchange interaction can be influenced by the temperature and the nature of the solvent, the EPR spectra give evidence of the dynamic behavior of the dendritic branches. FT-IR spectroscopy has revealed that a hydrogen-bonded network is formed between the amide functionalities of the end groups, consistent with the observed solvent effect on the EPR spectra.

V. Experimental Section

Synthesis. 3-[[(2,5-Dioxo-1-pyrrolidinyl)oxy]carbonyl]-2,2,5,5-tetramethyl-1-pyrrolidinyloxy (1). To a solution of 3-carboxy-2,2,5,5-tetramethyl-1-pyrrolidinyloxy (Aldrich, 203 mg, 1.09 mmol) in 1 mL of 1,2-dimethoxyethane were added *N*-hydroxysuccinimide (126 mg, 1.09 mmol) and 1,3-dicyclohexylcarbodiimide (247 mg, 1.20 mmol) upon cooling with an ice bath. After 1 h the reaction mixture was brought to room temperature and was allowed to react for an additional 12 h and subsequently filtered. The filtrate was evaporated to dryness under reduced pressure followed by two washings with hot cyclohexane (5 mL). After drying *in vacuo*, the ester was obtained as a yellow viscous oil (281 mg, 91%). The product was characterized in dichloromethane solution with FT-IR ($\nu_{C=O}$ = 1814, 1788, and 1744 cm^{-1}) and EPR (a_N = 14.49 G, a_C = 9.7 G, and a_C = 5.9 G).

3-[(1-Propylamino)carbonyl]-2,2,5,5-tetramethyl-1-pyrrolidinyloxy (2). Propylamine (0.5 mL, 6 mmol) was slowly added to a solution of 3-[[(2,5-dioxo-1-pyrrolidinyl)oxy]carbonyl]-2,2,5,5-tetramethyl-1-pyrrolidinyloxy (**1**) (71 mg, 0.25 mmol) in 2 mL of dichloromethane. After stirring for 4 h the reaction mixture was extracted with a saturated aqueous sodium carbonate solution. The organic phase was dried (Na_2SO_4) and evaporated to dryness *in vacuo*. Yellow needles were obtained after recrystallization in hexane (50 mg, 88%). The product was characterized in dichloromethane solution with FT-IR (ν_{N-H} = 3440 cm^{-1}, $\nu_{C=O}$ = 1677 cm^{-1}) and EPR (a_N = 14.49 G, a_C = 9.7 G, and a_C = 5.9 G).

DAB-*dendr*-(NH-3-CO-PROXYL)$_n$ (n = 2, 4, 8, 16, 32, 64). To a solution of DAB-*dendr*-$(NH_2)_n$ (0.56 mmol end groups) in 3 mL of dichloromethane was added 3-[[(2,5-dioxo-1-pyrrolidinyl)oxy]carbonyl]-2,2,5,5-tetramethyl-1-pyrrolidinyloxy (**1**) (161 mg, 0.57 mmol). After stirring for 12 h at room temperature,

an aqueous solution of 1 N sodium hydroxide was added and the two-phase system was stirred for an additional hour to hydrolyze the excess of activated ester. The two layers were separated, followed by a base extraction with a saturated aqueous sodium carbonate solution. The organic phase was dried (Na_2SO_4) and concentrated *in vacuo*, resulting in yellow glasses for each generation.

Pure DAB-*dendr*-(NH-3-CO-PROXYL)$_2$ was obtained in a yield of 84%. DAB-*dendr*-(NH-3-CO-PROXYL)$_4$ was purified using column chromatography (SiO_2; eluent, methanol) and obtained in a yield of 51%.

The second (n = 8) and the third (n = 16) generation PROXYL-functionalized dendrimers were purified by extraction from dichloromethane into an aqueous solution of 1 N hydrochloric acid. The aqueous layer was brought to pH > 10 and extracted with dichloromethane. This gave the functional dendrimers in a yield of 35% for the second and 38% for the third generation.

DAB-*dendr*-(NH-3-CO-PROXYL)$_{32}$ and DAB-*dendr*-(NH-3-CO-PROXYL)$_{64}$ were purified by dialysis (regenerated cellulose 24 Å) with dimethylformamide. Dialysis was continued until no further decrease in the EPR signal belonging to free 3-carboxy-PROXYL radicals compared to the broad signal of the functionalized dendrimer was observed. After removal of the solvent, the functionalized dendrimers were obtained in 28% yield for the fourth and 42% yield for the fifth generation.

The purity of all compounds was checked with FT-IR in dichloromethane solution by the absence of the N−H stretch vibrations belonging to unreacted primary amines and the C═O stretch vibrations belonging to the succinimic ester or the 3-carboxy-PROXYL.

MALDI-TOF mass spectrometry for n = 2 and 4 gave masses of 427.2 and 992.3 g/mol, respectively, without indication of lower molecular-weight dendrimers. For n = 8 the principal molecular peak was found at 2123.9 g/mol and fragmentation peaks at appeared at 1955.4, 1911.8, 1898.3, 1883.8, and 1786.9 g/mol. The MALDI-TOF mass spectrum for n = 16 gave the most abundant peak at 4386.9 g/mol and peaks assigned to fragmentation at 4146.9, 3906.9, 2221.1, and 1035.8 g/mol

Electron Paramagnetic Resonance. EPR spectra were recorded using a Bruker ER200D SRC spectrometer, operating with an X-band standard cavity and interfaced to a Bruker Aspect 3000 data system. Temperature was controlled by a Bruker ER4111 variable temperature unit between 100 and 400 K. Samples were flushed with He to remove molecular oxygen and kept under constant He atmosphere during measurements.

IR Spectroscopy. Infrared spectra were recorded on a Perkin-Elmer 1605 FT-IR spectrophotometer between 4400 and 450 cm^{-1} using a 1 mm pathway.

Acknowledgment. We would like to thank Dr. J. F. G. A. Jansen for performing preliminary experiments resulting in this investigation. Dr. H. J. Räder (Max Planck Institute, Mainz, Germany) is gratefully acknowledged for recording the MALDI-TOF mass spectra. This work was supported by the Netherlands Foundation for Chemical Research (SON) with financial aid from the Netherlands Organization for Scientific Research (NWO). DSM Research is acknowledged for an unrestricted research grant.

References and Notes

(1) Newkome, G. R.; Moorefield, C. N.; Vögtle, F. *Dendritic Molecules: Concepts, Synthesis, Perspectives*; VCH: Weinheim, 1996. Tomalia, D. A.; Naylor, M. A.; Goddard, W. A., III *Angew. Chem., Int. Ed. Engl.* **1990**, *29*, 138. Fréchet, J. M. J. *Science* **1994**, *263*, 1710.

(2) Wooley, K. L.; Hawker, C. J.; Fréchet, J. M. J.; Wudl, F.; Srdanov, G.; Shi, S.; Li, C.; Kao, M. *J. Am. Chem. Soc.* **1993**, *115*, 9836. Hawker, C. J.; Wooley, K. L.; Fréchet, J. M. J. *J. Chem. Soc., Chem. Commun.* **1994**, 925.

(3) Jin, R.-H.; Aida, T.; Inoue, S. *J. Chem. Soc., Chem. Commun.* **1993**, 1260. Sadamoto, R.; Tomioka, N.; Aida, T. *J. Am. Chem. Soc.* **1996**, *118*, 3978. Tomoyose, Y.; Jiang, D.-L.; Jin, R.-H.; Aida, T.; Yamashita, T.; Horie, K.; Yashima, E.; Okamoto, Y. *Macromolecules* **1996**, *29*, 5236.

(4) Dandliker, P. J.; Diederich, F.; Gross, M.; Knobler, C. B.; Louati, A.; Sanford, E. M. *Angew. Chem., Int. Ed. Engl.* **1994**, *33*, 1739.

(5) Hawker, C. J.; Wooley, K. L.; Fréchet, J. M. J. *J. Am. Chem. Soc.* **1993**, *115*, 4375.

(6) Nagasaki, T.; Ukon, M.; Arimori, S.; Shinkai, S. *J. Chem. Soc., Chem. Commun.* **1992**, 608. Nagasaki, T.; Kimura, O.; Ukon, M.; Arimori, S.; Hamachi, I.; Shinkai, S. *J. Chem. Soc., Perkin Trans 1* **1994**, 75.

(7) Xu, Z.; Moore, J. S. *Acta Polym.* **1994**, *45*, 83, and references therein.

(8) Jansen, J. F. G. A.; De Brabander-van den Berg, E. M. M.; Meijer, E. W. *Science* **1994**, *266*, 1226.

(9) Matyjaszewski, K.; Shigemoto, T.; Fréchet, J. M. J.; Leduc, M. *Macromolecules* **1996**, *29*, 4167.

(10) Racja, A.; Utamapanya, S.; Thayumanavan, S. *J. Am. Chem. Soc.* **1992**, *114*, 1884. Racja, A.; Utamapanya, S. *J. Am. Chem. Soc.* **1993**, *115*, 2396. Racja, A.; Utamapanya, S. *J. Am. Chem. Soc.* **1993**, *115*, 10688. Racja, A. *Chem. Rev.* **1994**, *94*, 871. Racja, A. *Adv. Mater.* **1994**, *6*, 605.

(11) Veciana, J.; Rovira, C.; Crespo, M. I.; Armet, O.; Domingo, V. M.; Palacio, F. *J. Am. Chem. Soc.* **1991**, *113*, 2552. Veciana, J.; Rovira, C.; Ventosa, N.; Crespo, M. I.; Palacio, F. *J. Am. Chem. Soc.* **1993**, *115*, 57. Ventosa, N.; Ruiz, D.; Rovira, C.; Veciana, J. *Mol. Cryst. Liq. Cryst. Sect. A.* **1993**, *232*, 333. Veciana, J.; Rovira, C. In *Magnetic Molecular Materials*; Gattechi, D., Kahn, O., Miller, J. S., Palacio, F., Eds.; Kluwer: Dordrecht, 1991, p 121.

(12) Nakamura, N.; Inoue, K.; Iwamura, H.; Fujioka, T.; Sawaki, Y. *J. Am. Chem. Soc.* **1992**, *114*, 1484. Nakamura, N.; Inoue, K.; Iwamura, H. *Angew. Chem., Int. Ed. Engl.* **1993**, *32*, 872. Matsuda, K.; Nakamura, N.; Inoue, K.; Koga, N.; Iwamura, H. *Chem. Eur. J.* **1996**, *2*, 259. Matsuda, K.; Nakamura, N.; Inoue, K.; Koga, N.; Iwamura, H. *Bull. Chem. Soc. Jpn.* **1996**, *69*, 1483.

(13) Miller, L. L.; Hashimoto, T.; Tabakovic, I.; Swanson, D. R.; Tomalia, D. A. *Chem. Mater.* **1995**, *7*, 9. Duan, R. G.; Miller, L. L.; Tomalia, D. A. *J. Am. Chem. Soc.* **1995**, *117*, 10783.

(14) Bryce, M. R.; Devonport, W.; Moore, A. J. *Angew. Chem., Int. Ed. Engl.* **1994**, *33*, 1761.

(15) Fillaut, J.-L.; Linares, J.; Astruc, D. *Angew. Chem., Int. Ed. Engl.* **1994**, *33*, 2460. Moulines, F.; Djakovitch, L. Boese, R.; Gloaguen, B.; Thiel, W.; Fillaut, J.-L.; Deville, M.-H.; Astruc, D. *Angew. Chem., Int. Ed. Engl.* **1993**, *32*, 1075.

(16) Alonso, B.; Morán, N.; Casado, C. M.; Lobete, P.; Losada, J.; Cuadrado, I. *Chem. Mater.* **1995**, *7*, 1440.

(17) Tenhu, K.; Sundholm, F. *Br. Polym. J.* **1990**, *23*, 129. Guyot, A.; Revillon, A.; Camps, A.; Monthéard, J. P.; Catoire, B. *Polym. Bull.* **1990**, *23*, 419. Pilar, J.; Horák, D.; Labský, J.; Švec, F. *Polymer* **1988**, *29*, 500. Wielema, T. A.; Engberts, J. B. F. N. *Eur. Polym. J.* **1988**, *24*, 647. Tsay, F. D.; Gupta, A. *J. Polym. Sci. B, Polym. Phys.* **1987**, *25*, 855. Rånby B. G.; Rabek, B. F. *ESR Spectroscopy in Polymer Research*; Springer: Berlin, 1977.

(18) Here, the expression DAB-*dendr*-$(NH_2)_n$ is also used for n = 2 to have a consistent notation within this homologous series of polyradicals, even though n = 2 does not correspond to a dendritic structure.

(19) De Brabander-van den Berg, E. M. M.; Meijer, E. W. *Angew. Chem., Int. Ed. Engl.* **1993**, *32*, 1308.

(20) Luckhurst, G. R. *Mol. Phys.* **1966**, *10*, 543. Luckhurst, G. R.; Pedulli, G. F. *J. Am. Chem. Soc.* **1970**, *92*, 4738. Luckhurst, G. R. In *Spin Labeling Theory and Applications*; Berliner, L. J., Ed.; Academic Press: New York, 1976; p 133.

(21) Glarum, S. H.; Marshall, J. H. *J. Chem. Phys.* **1967**, *47*, 1374.

(22) Parmon, V. N.; Zhidomirov, G. M. *Mol. Phys.* **1974**, *27*, 367. Parmon, V. N.; Kokorin, A. I.; Zhidomirov, G. M.; Zamaraev, K. I. *Mol. Phys.* **1975**, *30*, 695.

(23) Adievich, N. I.; Forbes, M. D. E. *J. Phys. Chem.* **1995**, *99*, 9960.

(24) Slichter, C. P. *Principles of Magnetic Resonance*; Harper and Row: New York, 1963.

(25) Cuadrado, I.; Morán, M.; Casado, C. M.; Alonso, B.; Lobete, F.; García, B.; Ibisate, M.; Losada, J. *Organometallics* **1996**, *15*, 5278.

(26) Jansen, J. F. G. A.; Peerlings, H. W. I.; De Brabander-van den Berg, E. M. M.; Meijer, E. W. *Angew. Chem., Int. Ed. Engl.* **1995**, *34*, 1206.

(27) Gardner, R. R.; Gellman, S. H. *J. Am. Chem. Soc.* **1995**, *117*, 10411. Gellman, S. H.; Dado, G. P.; Liang, G.-B.; Adams, B. R. *J. Am. Chem. Soc.* **1991**, *113*, 1164.

MA9701853